

## LONGSHORE VARIABILITY OF SWASH MOTION IN A DISSIPATIVE TOURISTIC BEACH FROM HIGH-FREQUENCY VIDEO IMAGERY

**Chatzipavlis A.\***, Chatzistratis D., Trygonis V., Monioudi I., Andreadis O., Psarros F.,  
Velegrakis A.F.

Department of Marine Sciences, School of the Environment, University of the Aegean, University Hill - 81100, Mytilene, Lesvos, Greece

### Abstract

Changes in beach morphology are frequent, varying from small to larger spatio-temporal scales, being subjected to the ever-changing hydrodynamic action. Swash zone motions have direct impact on beach morphology and are necessary parameters for appropriate coastal management and hazard mitigation. This study investigates spatio-temporal variability in swash motion and shoreline dynamics, which additionally are essential from regulatory boundaries for appropriate spatial planning of the beach zone. The traditional mapping techniques commonly lack the temporal resolution needed for accurate mapping of the swash zone dynamics. An autonomous coastal optical system was deployed at a dissipative, microtidal sandy beach (Marmari, Kos Island) and provided high-frequency hourly records of the shoreline and the wave run-up/run-down positions, simultaneously to a wave logger deployed offshore the beach. Results reveal significant variability in shoreline and wave run-up maximum, even under moderate incoming wave action. The system's automatization process is robust, capable in providing accurate morphological data, which are crucial for coastal planning.

**Keywords:** *wave run-up, swash zone dynamics, shoreline detection, coastal video monitoring*

\*Corresponding author: Chatzipavlis Antonis ([a.chatzipavlis@marine.aegean.gr](mailto:a.chatzipavlis@marine.aegean.gr))

### 1. Introduction

Swash zone dynamics play a crucial role in sediment transport, beach morphology, and nearshore circulation, making it essential to understand the spatio-temporal variability of the natural processes (e.g., Houser 2009; Suanez *et al.* 2016). Swash motion (in the zone between wave run-up and run-down) is controlled by several natural and artificial factors such as i) the wave characteristics; ii) sea level variability; iii) beach geo-morphology; and iv) the presence of technical structures at the beach face such as roads and sea walls (Splinter *et al.* 2010). The main morphological factors in this zone are the wave run-up maximum excursion, which refers to the maximum vertical distance reached by the wave action on the beach (e.g., Holman 1986), and the shoreline that defines the boundary between land and water and is dynamically influenced by sea level changes (tide or/and surge) and the wave excursion.

These morphological parameters are commonly used as reference lines in defining areas/set-back zones of absolute beach protection or/and building limitations. For instance, wave run-up maximum excursion (defined as the “aigialos” line in Greek legislation) is used to map and set a setback zone of no development/constructions according to the national law (Greek Law 2971/2001). Furthermore, several relevant European directives promote and suggest the definition of such zones (e.g., the Act on Coastal Protection (78/2017); the EU Directive 2014/52/EU; and the ICZM Protocol to the Barcelona Convention (Art. 8(2)). Regarding shoreline position, this is not only a basic indicator when examining beach erosion phenomena, but also used to define the carrying capacity (i.e., the number of people able to visit the beach simultaneously).

The definition of these crucial morphological factors is of paramount importance for coastal management, hazard mitigation, and sustainable development in coastal areas, which should be based on accurate and long-term records of appropriate spatio-temporal coverage. However, the traditional mapping techniques are not able to cope with this issue satisfactorily. Satellite image timeseries cannot provide high temporal resolution, as images are dependent from the satellites' orbit and other physical restrictions such as cloudiness. LiDAR flights do not only have increased cost but also require dedicated human effort, while UAVs (drones) are not able to fly during intense wind activity (typically the case when most morphological changes take place at the beach). Finally, repeated topographic mapping through ground-based geomatic instrumentation, such as Real-time Kinematic positioning systems (RTKs), require incredible amount of time and human effort (especially during storm events).

It is evident that nearshore hydro-morphodynamic processes are based on complex forcing-response mechanisms operating at various spatio-temporal scales (Suanez *et al.* 2016) that have not yet been completely understood. To resolve this, coastal scientists use/develop numerical simulations or/and empirical formulae that parameterize the swash dynamics (e.g., Roelvink *et al.* 2010; Samaras & Karambas, 2024). Shoreline position is estimated through widely accepted methodologies (e.g., the Bruun rule (Bruun 1954) and the EBP method (Dean

1990)), whereas the estimation of wave run-up excursion is based on theoretical formulae that suggest that the excursion is controlled by the incident wave energy and the nearshore seabed slope (e.g., Holman 1986; Stockdon *et al.* 2006). The traditional numerical modeling techniques, not only require a large number of input parameters measured in the field (topo-bathymetric, granulometric and hydrodynamic data), but are also based on the calibration process (i.e., validation of the model projections/output with real recorded conditions). The latter highlights the need of retrieving accurate morphological information, during the simulated events.

Over the last years, coastal based video cameras have proved to be a valuable tool for recording in detail the spatio-temporal variations in the swash zone, allowing for comprehensive analysis of beach dynamics, while effort has been given towards the development of image processing algorithms that are capable to record with high accuracy specific coastal features of interest on specialized optical datasets deriving from coastal video monitoring systems (e.g., Velegrakis *et al.* 2016).

## 2. Methodology

Marmari is a highly touristic beach located at the northern part of Kos Island, 15 km west of Kos town. This microtidal dissipative beach is characterized by smooth slopes, fine sediments and the presence of a longshore sandbar, whose position varies depending on the incoming hydrodynamic action. Marmari is very popular for surfing activities, while many hotels and other recreational facilities are present at the backshore of the beach, which over the last decades is experiencing erosional phenomena.

An autonomous Beach Optical Monitoring System (BOMS) was installed at the roof of a hotel (Stella Maris, Easting: 512996.60 m UTM, Northing: 4081583.83 m) at an elevation of 10 m, while a wave logger (RBR|*Virtuoso*) was deployed at a depth of 7.9 m offshore (Figure 1a). The BOMS installed in Marmari consists of a station PC and one PointGrey FLEA-2 video camera, set to obtain high-resolution hourly videos with a sampling rate of 5 Hz for 10 minutes during daylight (i.e., 3,000 frames per hour). During the remaining 50 minutes two main tasks are scheduled to the station PC. First, all frames/images are corrected for lens distortion and furthermore processed by using standard photogrammetric methods and accurate positions of Ground Control Points (GCPs), collected with a Differential GPS (Topcon Hipper RTK-DGPS). Second, the recorded hourly frames are furthermore processed to produce metadata (optical products) consisting of one IMMAX and one TIMEX image per hour, amongst others (for details see Velegrakis *et al.* 2016). IMMAX images are the result of the maximum pixel intensity of all images, and thus are capable of capturing the contrast between the maximum wave excursion towards inland (wave run-up maximum) (Figure 1b and 1c). TIMEX images are the result of the average pixel intensity and are used to extract the shoreline position. Thus, in this case the location of the shoreline is considered as the mean position of the swash motion during the recording cycle.

Within the framework of the MARICC project ([www.maricc.gr](http://www.maricc.gr)), IMMAX and TIMEX timeseries were recorded for the energetic winter - spring period between 12/11/2022 - 06/04/2023. However, there have been specific cases when the camera lens was covered by salt sheet (deriving from sea spray during specific storm events) and for which optical data were not available. Two automatic detectors were applied to extract the longshore positions of the wave run-up maximum and the shoreline, on each of the hourly recorded IMMAX and TIMEX images, respectively. Both detectors are based on an algorithm using a localized kernel that progressively grows along the TIMEX and IMMAX digital image, following the high intensity zone along the feature of interest (Velegrakis *et al.* 2016; Chatzipavlis *et al.* 2018). Manual corrections were performed to the automatically extracted positions with the use of a specifically developed software/code in MATLAB. The accuracy of the records decreases with the distance from the camera due to the increasing pixel footprint, that is also dependent from the elevation of the camera. Lower elevation points result to narrower field of view compared to camera deployment at higher elevation. For this reason, detections from the proximal beach stretch (550 m long – Figure 2a) were considered for analysis. For this section of the beach, the pixel footprint and the accuracy of detections are estimated at about 0.25 m. The maximum shoreward movement of each longshore beach point of all the hourly detected/recorded shoreline and wave run-up maximum positions for the monitored beach stretch, has been extracted in order to investigate the long-term morphological behavior. In addition, the movement/variability of six equally-spaced (every 70 m) longshore locations was taken into consideration (Figure 1c), as indicators of the temporal evolution of the beach, compared to the morphological condition of the starting day of the monitoring period.

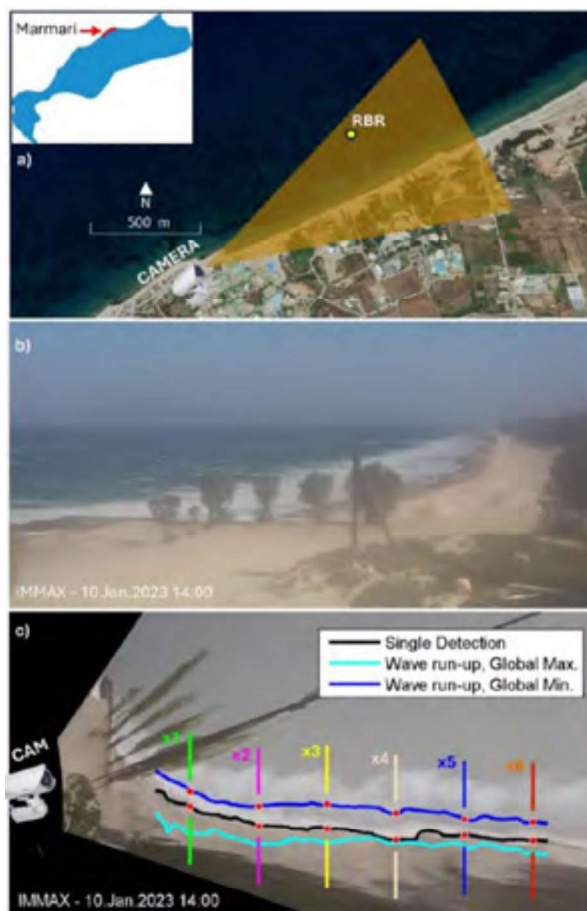


**Figure 1. a)** Positions of the video camera and the wave logger (RBR) deployed in Marmari beach at 7.9 m depth. **b)** Example of an IMMAX image produced from the video (frames) analysis for a specific date. **c)** The same IMMAX image after rotation by setting the position of the camera as central (0,0) point. The six equally-spaced (70 m from each other) longshore positions, selected for further analysis, are also shown.

### 3. Results

Shoreline and wave run-up maximum positions were found to vary significantly during the monitoring period. More specifically, the shoreline of the monitored beach stretch was found to range between 12 and 16 m (Figure 2a and 2b), while wave run-up maximum positions were found to range between 11 and 24 m (Figure 2c). The central and eastern sectors of the beach (between  $x = 300$  m and  $x = 550$  m) were found to have lower standard deviations, and thus be slightly more stable compared to the western sector (between  $x = 150$  m and  $x = 300$  m). It is important to note that the higher swash maxima variability is found at the central sector of the beach (between  $x = 270$  m and  $x = 350$  m), which is not consistent with the locations of the highest recorded shoreline variability (found between  $x = 370$  m and  $x = 450$  m). The latter could be attributed to the nearshore hydrodynamic circulation, and more possibly to longshore sediment transport processes. Also, high morphological variability is evident at the western edge of the monitored beach (between  $x = 150$  m and  $x = 200$  m), which is delimited from a dike at the location where four trees are also present (see also Figure 1b).

When the temporal evolution of the six selected longshore locations is examined, compared to the starting day of the optical records, specific morphological patterns are evident. Both shoreline and wave run-up maximum positions in these locations are found to be triggered by the wave action. In periods of increased wave heights (more than 0.5 m) approaching from offshore (e.g., at 22/11, 12/12, 11/01 and 12/03; see Figure 2f), wave run-up maximum and shoreline positions at the six selected locations were found to be significantly displaced, compared to the previous day (Figure 2e and 2d, respectively). For instance, at most of the selected locations shoreline was found to be displaced by about 6 m, 4 m, 4 m and 2 m at 22/11, 12/12, 11/01 and 12/03, compared to the previous day, respectively (Figure 2d). For the same days, max. wave run-up displacement was found to be of about 8, 4 m, 9 m and 4 m, respectively. It has to be noted that all selected longshore locations follow similar erosion/accretion

patterns, controlled by swash motion. However, location x1 (green line) showed increased erosional behavior (and increased corresponding swash motion towards inshore) after the energetic wave event ( $H_s = 0.8$  m) occurred on 22/11. Also, location x4 (at  $x = 395$ ) was found to have the highest shoreline retreat (-12 m) of the examined longshore locations, compared to the starting period of the optical records.

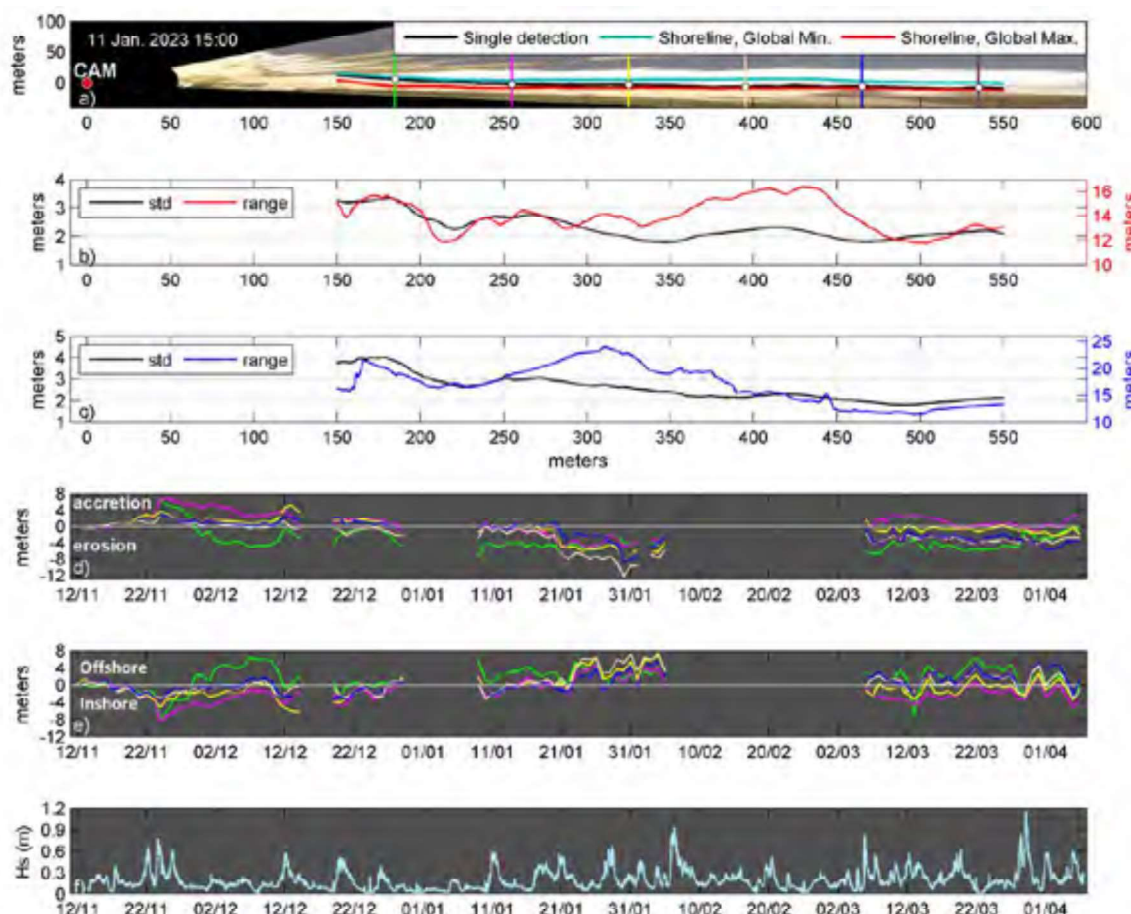


**Figure 2.** a) Geo-rectified TIMEX mosaic of the monitored section in Marmari beach, showing also the locations of the six selected profiles; black line denotes the shoreline detection on the plotted TIMEX mosaic, whereas red and cyan lines depict the maximum and minimum inshore positions of the shoreline during the monitoring period. b) Spatial distributions of the standard deviation and range of the longshore shoreline position and c) wave run-up maximum. d) Temporal changes in shoreline position and e) wave run-up maximum, at the six selected locations, relative to the starting date of the monitoring period (accretion/erosion). f) Time series of significant wave height recorded from the wave logger.

The minimum and maximum detected shoreline positions for the monitoring period are depicted in Figure 2a, while the minimum and maximum detected wave run-up positions (i.e., the “aigialos line” in Greek legislation for the monitoring period) are depicted on Figure 1c. The recorded significant spatio-temporal variability of these crucial morphological parameters reveals the main advantage of the BOMS against the rest of the mapping techniques, which are lacking such high frequency records.

### 3. Discussion and Conclusions

Swash motion of the monitored stretch of Marmari beach was found to be highly variable during the monitoring period, triggered by the wave action. The wave climate offshore the beach (at 7.9 m depth) was found to be moderate, with most of the recorded significant wave height values being below 0.6 m during the 5-month energetic winter-spring monitoring period. However, under these conditions of wave forcing, the beach system was found to be vulnerable to intense morphological changes. Shoreline and wave run-up maximum excursion

ranged between 12-16 m and 11-24 m, respectively. Sectors of highest variability are different for shoreline and swash maximum, attributed to longshore hydrodynamic and sediment transport processes, concerning also i) the fine sedimentology of the beach, and ii) the varying position of the longshore sandbar that defines the wave breaking zone at the nearshore.

The automated approach developed to extract shoreline and wave run-up maximum positions from TIMEX and IMMAX images proved to be a robust and efficient tool in resolving beach variability in fine spatio-temporal scales. Both positions are of high importance for coastal planners and engineers, as they form fundamental parameters of the swash zone dynamics, while at the same time, these morphological parameters form regulatory boundaries. A significant result of the present work is the development of an objective, robust and cost-effective methodology to define such coastal regulatory boundaries. The latter are of critical importance as they can define with high precision the “aigialos line” (in the long-term), a most crucial parameter for coastal planning. It has to be noted that detections presented in this work are focused at the proximal beach stretch, due to the increased pixel footprint in these areas, and thus, the results are characterized by very high accuracy. However, when it comes to the definition of set-back zones, detections of lower accuracy could be also used, and thus, longer beach sections can be monitored. Finally, such precise and high frequency shoreline and wave run-up positions, followed by simultaneous hydrodynamic records are valuable for accurate calibration/validation of the modeling techniques, used to resolve coastal morphodynamics.

### Acknowledgements

This research was conducted within the framework of the MARICC project (maricc.gr), supported by the Hellenic Foundation for Research and Innovation (H.F.R.I.) under the “2nd Call for H.F.R.I. Research Projects to support Post-Doctoral Researchers” (Project Number: 211).

### References

- Bruun P. (1954). Coast erosion and the development of beach profiles. Technical Memorandum, vol. 44, Beach Erosion Board, Corps of Engineers, 82 pp.
- Chatzipavlis A., Tsekouras G.E., Trygonis V., Velegrakis A.F., Tsimikas J., Rigos A., Hasiotis Th., Salmas C. (2018). Modeling beach realignment using a neuro-fuzzy network optimized by a novel backtracking search algorithm. *Neural Computing and Applications*, 17 pp. doi: 10.1007/s00521-018-3809-9.
- Dean R.G. (1990). Equilibrium beach profiles: characteristics and applications. *Journal of Coastal Research*, 7, 53-84.
- Greek Law 2971/2001: "Regime for the protection of the sea area, the shores of the sea, the environment and other provisions." (ΦΕΚ Α' 194/10.9.2001) as amended by Law 3584/2007 (ΦΕΚ Α' 65/16.4.2007), Law 4256/2014 (ΦΕΚ Α' 110/24.6.2014), and Law 4546/2018 (ΦΕΚ Α' 153/25.9.2018).
- Holman R.A. (1986). Extreme value statistics for wave run-up on a natural beach. *Coastal Engineering*, 9(6), 527–544. doi: 10.1016/0378-3839(86)90002-5.
- Houser C. (2009). Synchronization of transport and supply in beach-dune interaction. *Progress in Physical Geography*, 33(6), 733–746. doi: 10.1177/0309133309350120.
- Samaras A.G., Karambas T.V (2024). Simulating Erosive and Accretive Conditions in the Swash: Applications of a Nonlinear Wave and Morphology Evolution Model. *Journal of Marine Science and Engineering* 12, 140.
- Roelvink D., Reniers A.J.H.M., Van Dongeren A., Van Thiel de Vries J., Lescinski J., McCall R. (2010). XBeach model description and manual. Unesco-IHE Institute for Water Education, Deltares and Delft University of Technology. Report June, 21, 2010.
- Splinter K. D., Turner I. L., Davidson M. A. (2010). Swash zone sediment transport across the surf zone in large-scale laboratory experiments. *Journal of Geophysical Research: Earth Surface*, 115(F3), 1-14.
- Stockdon H.F, Holman R.A, Howd P.A., Sallenger J.A.H. (2006). Empirical parameterization of setup, swash, and runup. *Coastal Engineering* 53(7):573–588. doi: 10.1016/j.coastaleng.2005.12.005.
- Suarez S., Blaise E., Cancouet R., Floch F. (2016). Empirical parameterization of wave run-up and dune erosion during storm conditions on a natural macrotidal beach. *Journal of Coastal Research*, SI75, 932-936.
- Velegrakis A.F., Trygonis V., Chatzipavlis A.E., Karambas T., Vousdoukas M.I., Ghionis G., Monioudi I.N., Hasiotis T., Andreadis O., Psarros F. (2016). Shoreline variability of an urban beach fronted by a beachrock reef from video imagery. *Natural Hazards* 83(1), 201–222. doi: 10.1007/s11069-016-2415-9.